JACS
JOURNAL OF THE AMERICAN CHEMICAL SOCIETY
Article
pubs.acs.org/JACS

Oxidation Half-Reaction of Aqueous Nucleosides and Nucleotides via Photoelectron Spectroscopy Augmented by ab Initio Calculations

Christi A. Schroeder,[†,#] Eva Pluhařová,[‡,#] Robert Seidel,[†] William P. Schroeder,[†] Manfred Faubel,[§] Petr Slavíček,*[,∥] Bernd Winter,*[,⊥] Pavel Jungwirth,*[,‡] and Stephen E. Bradforth*[,†]

[†]Department of Chemistry, University of Southern California, Los Angeles, California 90089-0482, United States

[‡]Institute of Organic Chemistry and Biochemistry, Academy of Sciences of the Czech Republic, Flemingovo nám. 2, 16610 Prague 6, Czech Republic

[§]Max-Planck-Institut für Dynamik und Selbstorganisation, Bunsenstrasse 10, D-37077 Göttingen, Germany

[∥]Department of Physical Chemistry, Institute of Chemical Technology, Technická 5, 16628 Prague 6, Czech Republic

[⊥]Institute of Methods for Material Development, Helmholtz Center Berlin, Albert-Einstein-Strasse 15, D-12489 Berlin, Germany

Supporting Information

ABSTRACT: Oxidative damage to DNA and hole transport between nucleobases in oxidized DNA are important processes in lesion formation for which surprisingly poor thermodynamic data exist, the relative ease of oxidizing the four nucleobases being one such example. Theoretical simulations of radiation damage and charge transport in DNA depend on accurate values for vertical ionization energies (VIEs), reorganization energies, and standard reduction potentials. Liquid-jet photoelectron spectroscopy can be used to directly study the oxidation half-reaction. The VIEs of nucleic acid building blocks are measured in their native buffered aqueous environment. The experimental investigation of purine and pyrimidine nucleotides, nucleosides, pentose sugars, and inorganic phosphate demonstrates that photoelectron spectra of nucleotides arise as a spectral sum over their individual chemical components; that is, the electronic interactions between each component are effectively screened from one another by water. Electronic structure theory affords the assignment of the lowest energy photoelectron band in all investigated nucleosides and nucleotides to a single ionizing transition centered solely on the nucleobase. Thus, combining the measured VIEs with theoretically determined reorganization energies allows for the spectroscopic determination of the one-electron redox potentials that have been difficult to establish via electrochemistry.

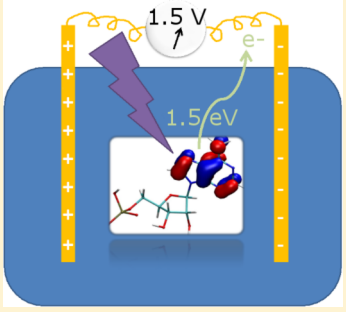

INTRODUCTION

Oxidative damage induced by ionizing radiation has significant deleterious effects on genomic DNA, such as strand breaks and nucleobase damage,[1] which can lead to mutations and cancer.[2] Double strand breaks are by far the most damaging lesion as their repair is particularly difficult and the mutation probability is high.[3] For a double strand break to occur, at least two oxidative lesions must lie within close range on the double helix and the probability of such an occurrence increases if the hole (the locus of the oxidized base) can migrate efficiently by charge transport.[4−8] Rates of electron (hole) transport between two nucleobases are determined by Marcus theory.[9] To predict such rates, accurate knowledge of two key energetic parameters is required: the energy change for the electron to move between nucleobases and the total reorganization energy connected with this process. Equivalently, this information can be synthesized from knowledge of the energetic parameters for the redox half-reactions of the two individual nucleobases, namely the vertical ionization energies (VIEs) of each and the individual reorganization energies on loss of an electron.[10] Likewise, the long-lived electronically excited states populated after ultraviolet exposure of DNA in sunlight have recently been shown to involve charge transfer between adjacent bases; the energetic availability of such charge transfer states is determined by knowledge of the VIE of the electron donor nucleobase as well as the electron affinity of the accepting base.[11−13] Despite the severe consequences of damage to DNA by ionizing or ultraviolet radiation, and the growing interest in DNA as a scaffold for electronic materials,[14,15] reliable energetic information of this sort has been difficult to come by for native nucleobases.

A general consensus in the literature on the standard one-electron redox potentials of the nucleobases has not yet been reached.[16,17] Measuring the redox properties of these molecules by electrochemical means is complicated by their dependence on protonation equilibria (giving pH dependent shifts in half-potentials) and their tendency to undergo rapid deprotonation and further follow-up reactions after oxidation.[18,19] Time-resolved experiments have indicated that the initial charge transfer step (removal of an electron) is in fact not dependent upon pH,[20] but the slower subsequent follow-up reactions can

Received: August 8, 2014
Published: November 27, 2014

DOI: 10.1021/ja508149e
J. Am. Chem. Soc. 2015, 137, 201−209

result in irreversible charge transfer at a measurement electrode surface.[21,22] These poorly defined follow-up reactions influence the redox equilibrium, resulting in irreversible conditions that can artificially lower the measured redox potential by as much as 0.3 V.[17]

In an effort to eliminate the complications that arise due to protonation equilibria, Seidel et al. performed a series of cyclic voltammetry experiments to electrochemically probe the oxidation potential of nucleosides (more formally, the standard reduction potential of the nucleoside radical cation, $E^0(N^{\bullet+}/N)$) in acetonitrile.[16] However, experimental traces revealed that even under aprotic conditions, redox reactions were still irreversible for all nucleosides. As such, the resulting electrochemically measured values represent a lower limit of the potentials for the nucleosides.[17] Steenken and co-workers circumvented the problem of irreversible redox reactions in water by measuring aqueous electron transfer equilibria between purine nucleosides and a reference molecule with a well-defined reduction potential to derive the nucleoside radical cation reduction potential. Although values for purines are established, estimates for the pyrimidine nucleosides by this approach are considerably less certain.[23]

This overall situation is hardly satisfactory. The best experimental data comparing all five bases are not from an aqueous solution. Moreover, these values are in relatively poor agreement with experimental measurements in water that require multiple corrections to be transformed into numbers suitable for modeling electron transfer processes between bases in aqueous solution.[24] Into this void, there have been recent attempts to provide such data from first-principles theory using free energy cycles.[17,24] The most recent and comprehensive potential estimates for the nucleobases are from Schlegel and co-workers; however, their computations for redox potentials are not in quantitative agreement with experimental values in aqueous solutions and suggest that $E^0(N^{\bullet+}/N)$ values in water should not differ much from those in the aprotic acetonitrile.[24] Finally, it is not clear how relevant these estimates are to the thermodynamic driving forces for charge transfer between stacked bases inside the different electrostatic environment of double helical DNA. Electronic interactions due to base stacking or hydrogen bonding inside the double helix have been predicted to result in shifts in the vertical ionization energies.[17,25,26] How large such shifts are for nucleobase ionization energies within the double helix is the topic of a recent paper by Cauet et al., who suggest a surprisingly steep increase (approximately 3.4 eV) in the nucleobase VIE due to long-range ordering of counterions along the phosphate backbone.[27] However, our most recent calculations, in which the effects of the aqueous environment were carefully included, paint a very different picture: water and counterions reduce the effect of the DNA environment on the VIE of nucleobases to ~0.1 eV.[28] It is clear that a direct experimental probe of the ionization energetics of the component molecular groups within aqueous DNA and a systematic assessment of what factors influence the ionization energies are highly desirable.

Gas phase and microhydrated nucleic acid components' IE values are pervasive in the literature,[29,30] yet much controversy exists regarding the energetic ordering of the highest lying orbitals and in particular the molecular orbital that is home to the least tightly bound electron.[31−33] Strong changes in the lowest gas phase IE are found when a negatively charged phosphate is included to make a nucleotide.[31] However, gas phase studies are of limited value in that they neglect dielectric contributions by the solvent to the electron binding energy (BE) as well as hydrogen bonding and counterion effects. The ability to measure the electron BEs of biomolecules in a native environment is crucial for obtaining a clear picture of the impact of the solvent and counterions. Here we present a complete study on the photoionization energies of the individual components of nucleic acids in buffered aqueous solutions.

METHODS

Experimental Section. Photoemission measurements were made at the U41 PGM undulator beamline at the BESSY synchrotron facility in Berlin. Valence photoelectron spectra were collected using 200 eV X-rays irradiating a 21 μm diameter liquid microjet flowing at a velocity of 60 m/s and a starting temperature of 20 °C. The jet temperature in the interaction region is not expected to be less than approximately 3 °C as determined by evaporative cooling modeling.[34,35] Experimental details of the liquid microjet technique have been previously described[36] and additional details can be found in the Supporting Information.

To generate meaningful data for the biomolecules studied, all samples were prepared in a buffer solution. Tris (tris(hydroxymethyl)-aminomethane) along with hydrofluoric acid (HF) was used to buffer and adjust the pH. More common biochemical buffers such as phosphate or Tris/HCl were avoided as they would yield significant contributions to the PE spectrum in the energy range under study arising from the phosphate or chloride anions, respectively.[37,38] We refer to the Supporting Information for a detailed description of the sample preparation.

Computational Methods. The ground state geometries of canonical forms of nucleobases, nucleosides, and nucleotides (both monovalent and divalent) in the most populated conformation in solution were optimized at the MP2/aug-cc-pVDZ level employing the polarizable continuum model (PCM) for the aqueous solvent. For AMP and UMP (both monovalent and divalent), we also optimized several structures with Na^+ counterions. The lowest VIE was calculated by employing the unrestricted version of the MP2 method with annihilated higher spin components via Schlegel's projection method (PMP2) for solute geometry before ionization. To model VIEs, we employed the nonequilibrium version of PCM (NEPCM), which means that only the fast component of the solvent response (corresponding to electronic motions) was included. This approach was shown to yield very good agreement with VIEs from photoelectron spectroscopy for a range of neutral and monovalent solutes including DNA components.[32,39] (Note that the standard PCM with both slow nuclear and fast electronic response included is suitable for the adiabatic ionization energy (AIE) rather than VIE calculations.) Ionization energies originating from more tightly bound electrons were obtained by adding the electronic excitation energies of the lowest ionized state, evaluated by employing the TDDFT with the BMK functional combined with NECPM, to the lowest VIE. This approach employing a well-chosen hybrid functional was shown to be a reliable way for calculating higher ionization energies of DNA components in refs 32 and 39. All calculations are performed with Gaussian 03.[40]

RESULTS AND DISCUSSION

Photoelectron Spectra. In general, because photoelectron (PE) spectroscopy ionizes solute and solvent molecules with near equal probability,[36] we find a solute concentration of at least 0.2 M is required to obtain an adequate signal-to-noise ratio when removing the aqueous buffer background (see the Supporting Information for procedure and Figure S2). The few millimolar solubility of nucleobases in water[41] has precluded us from studying nucleobases with the current experimental setup. As the pentose sugars substantially increase solubility, we were able to obtain high-quality PE spectra for the pyrimidine

DOI: 10.1021/ja508149e
J. Am. Chem. Soc. 2015, 137, 201−209

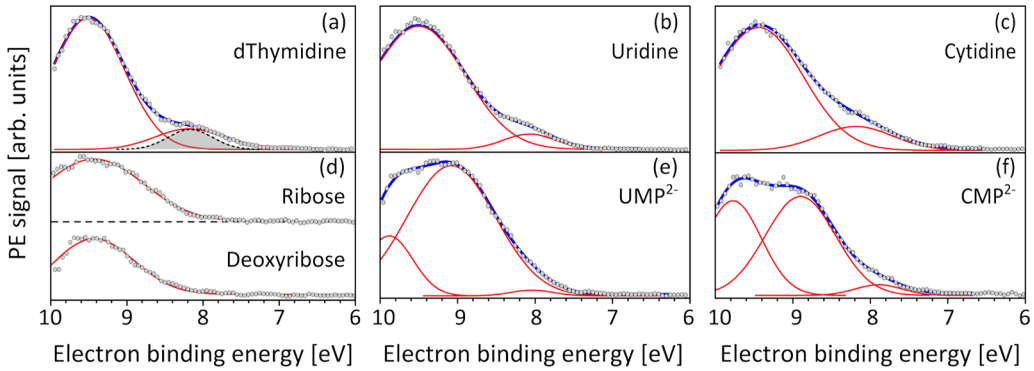

Figure 1. Differential spectra (shaded circles) and fits (overall fit, blue; individual Gaussians, red) for sugars, pyrimidine nucleosides, and pyrimidine nucleotides: (a) 0.4 M deoxythymidine, pH 7.5 [black dotted gray-shaded Gaussian: lowest binding energy peak fit with constrained fwhm of 0.62 eV (see text)]; (b) 1 M uridine, pH 7.1; (c) 0.7 M cytidine, pH 7.4; (d) 1 M D-ribose, pH 5.3 and 1 M deoxy-D-ribose, pH 5.5; (e) 0.9 M UMP^{2-}, pH 8.0; (f) 0.7 CMP^{2-}, pH 8.0.

nucleosides deoxythymidine, uridine, and cytidine (Figure 1a–c) after subtracting the background spectrum (1 M Tris–HF buffer) from the similarly buffered nucleoside solution. The photon energy was 200 eV. We have previously reported preliminary data on the ionization energies for deoxythymidine and cytidine.[32] However, repeating both experiments here using supersaturated solutions and higher energy resolution results in a significant improvement in signal-to-noise; in addition, the new PE spectrum of uridine completes the pyrimidine nucleoside family. All three exhibit similar spectral features consisting of two distinct bands, which are well fit by a sum of two Gaussians with the same band centers for the three investigated species. The difference resides in the intensity of the two bands; the lower BE peak is best resolved in deoxythymidine followed by uridine.

Figure 1d shows the PE spectra for D-ribose and 2′-deoxy-D-ribose. Both sugar solution spectra exhibit similar broad bands that can be fitted to a single Gaussian centered at 9.4 eV, although we cannot infer from this that the band represents ionization from a single orbital. Nevertheless, the lowest energy band at 8.1 eV in the nucleoside data is distinctly absent in the ribose and deoxyribose spectra, strongly suggesting the ionizing transition(s) associated with the 8.1 eV band in Figure 1a–c are solely attributable to orbital(s) on the nucleobase, as also shown computationally in our previous studies.[32,39] Given the similarity in peak positions, the sugar presumably contributes significantly to the 9.4 eV band in the nucleoside PE spectra. This interpretation is supported by poorer signal-to-noise ratio spectra (Supporting Information, Figure S3) of the most soluble of the nucleobases, cytosine. The spectrum shows approximately equal intensity between 8.0 and 9.5 eV BE, suggesting the cytosine base contributes intensity to the 9.5 eV band of the cytidine nucleoside as well as around ∼8.1 eV. Table 1 summarizes our findings for the valence region of cytidine, deoxythymidine, and uridine. Solubility constraints made acquisition of purine nucleoside PE spectra impossible, although recently Lübcke and co-workers have been able to extract an adiabatic ionization energy for adenosine using resonant multiphoton ionization from a liquid jet.[42] Solubilities for adenosine and guanosine, 30 and 2 mM,[41,43] respectively, are well below the ∼200 mM threshold required for adequate contrast to the water background in our experiments.

Next in the series of nucleic acid building blocks is the nucleotide, where the addition of orthophosphate at the 5′ position of the pentose sugar introduces a new low binding energy center and imparts a net negative charge to the molecule. Inorganic phosphate with a pK_{a2} of 7.2[44] has two protonation states ($H_2PO_4^-$ and HPO_4^{2-}) relevant to biological media. We have recently reported PE measurements of sodium phosphate solutions and find the lowest VIEs of 9.5 eV for $H_2PO_4^{1-}$ and 8.9 eV for HPO_4^{2-}.[37] The divalent phosphate contribution can be seen in the photoelectron spectra of the pyrimidine nucleotides UMP^{2-} and CMP^{2-} in Figure 1e,f. When we compare the pyrimidine nucleosides to nucleotides, it is apparent that the addition of the orthophosphate results in new PE intensity near 9 eV, reducing the ability to resolve the lower and higher energy peaks as distinct features. Gaussian fitting, however, suggests the lowest energy peak position and, therefore, the base electronic structure, remains essentially unaffected despite the addition of the charged phosphate near the nucleobase group. The omission of the last pyrimidine nucleotide, dTMP, in this data set is due to prohibitive cost of the compound at the multigram quantities required for each experimental run.

Table 1. Peak Centers of Electron Binding Energy (eV) Based on Gaussian Spectral Fitting Shown in Figure 1[a]

ribose	deoxyribose	uridine	deoxythymidine	cytidine
		8.1	8.1	8.1
9.4	9.4	9.5	9.5	9.4

[a]Similar binding energy peaks are aligned to suggest band assignments. The lowest ionization energies of the three pyrimidine nucleosides are equal within experimental error (±0.1 eV). The error in peak centers above 9 eV is larger due to distortion of peak shapes due to water displacement (see text).

The spectra of the purine nucleotides AMP^{2-} and GMP^{2-} are shown in Figure 2. Unlike the pyrimidine nucleotides, in which the lowest VIEs were nearly identical, there is an obvious difference in the AMP^{2-} and GMP^{2-} spectra between 6 and 8 eV. The first GMP^{2-} band begins to grow in at a lower energy than that of AMP^{2-} and peaks at 7.3 eV compared to 7.6 eV for AMP^{2-} (Table 2). We also note here that, even though some G-quadruplex formation and base stacking can be expected at concentrations as high as 1 M, an experimental concentration dependence study for GMP (Figure S6 in the Supporting Information) showed little or no change for the peak center of the low BE band and, therefore, the VIE. Specifically, over the concentration range studied (0.2–1 M), the fraction of free GMP decreases from ∼85 to 70%;[45] nevertheless, the free

DOI: 10.1021/ja508149e
J. Am. Chem. Soc. 2015, 137, 201–209

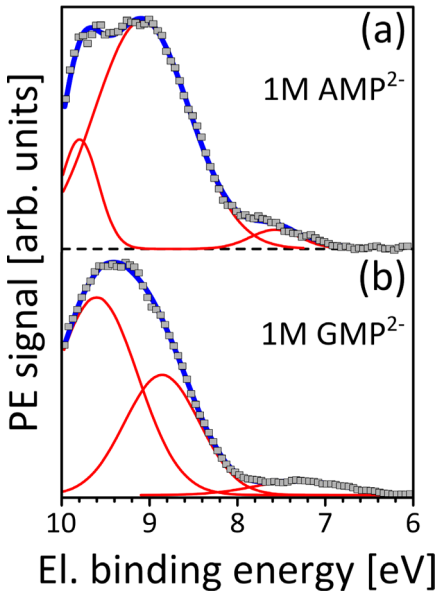

Figure 2. Purine nucleotide valence band photoelectron spectra (symbols) with Gaussian fits (overall fit, blue; individual peaks, red): (a) 1 M AMP^{2-}, pH 8.4; (b) 1 M GMP^{2-}, pH 8.1. Purine nucleotides show a significantly lower IE in the lowest electron binding energy band, with the first VIE of GMP^{2-} shifted to a lower binding energy than that of AMP^{2-}.

Table 2. Peak Centers of Electron Binding Energies (eV) for Pyrimidine and Purine Nucleotides Shown in Figure 2 Compared to the Peak Center of Inorganic Phosphate[a,37]

$H_2PO_4^{1-}$	HPO_4^{2-}	UMP^{2-}	CMP^{2-}	AMP^{2-}	GMP^{2-}
		8.0	7.9	7.6	7.3
9.5	8.9	9.1	8.9	9.1	8.9
		9.9	9.8	9.8	9.7

[a]Similar binding energy peaks are aligned to suggest band assignments. The lowest vertical ionization energies of the nucleotides have an experimental error (±0.1 eV). The error in peak centers above 9 eV is larger due to distortion of peak shapes due to water displacement (see text)

nucleotide is still the dominant species in the present experiments. At higher BEs, the overall band shapes are qualitatively similar to each other, as well as to those of the pyrimidine nucleotides. In Figure S4 in the Supporting Information we explore the effect of changing the protonation state of the adenine mononucleotide $AMP^{1-/2-}$. The spectra are nearly identical in the low-energy band centered at approximately 7.6 eV. Differences only become apparent at BEs greater than 8 eV; the higher energy feature appears shifted to lower energy in the deprotonated forms compared to the energy feature in the higher protonation state of the nucleotide. A similar shift in the higher energy feature is found for the different protonation states of an inorganic phosphate ion.[37] Importantly, there are no significant changes in the lowest binding energy band (i.e., the VIE) on changing the phosphate charge (via the pH).

Overall, these experimental findings provide evidence to suggest that in the aqueous solution each nucleic acid constituent group (base, sugar, phosphate) contributes individually to the photoelectron spectra, generating an overall spectrum arising as a sum over the individual parts. For nucleotides in particular, the presence of the high-dielectric solvent along with associated sodium counterions appears to screen the electrostatic interactions between the charged phosphate and the remainder of the molecule.

Comparisons of VIEs and Photoelectron Spectra to Theory. The broad nature of the spectral features makes it impossible to determine the number of states contributing to each band as well as the molecular identity of the originating orbitals solely from the experimental data. For this we seek the assistance of theory. Detailed theoretical results for pyrimidine nucleobases, nucleosides, and nucleotides have been reported previously.[32] The lowest vertical ionization energies for purines were separately considered in some detail and we explored whether broadening in the lowest BE photoelectron band could arise from various base tautomeric and conformational isomers.[39] However, the full liquid PE spectrum was not modeled and the effect of counterions or the protonation state has not been addressed theoretically hitherto. The computational approach we employ, along with the NEPCM treatment of the solvent environment, has been justified in detail by comparison to experimental and higher level ab initio

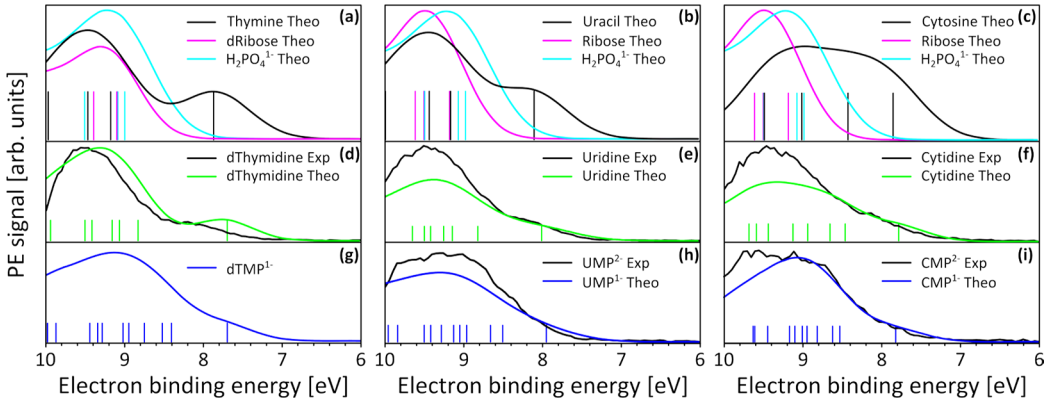

Figure 3. Decomposing the experimental and computed theoretical spectra for the pyrimidine nucleotides. Computed spectra for nucleobases (black), pentose sugars (magenta), and singly charged phosphate (cyan) shown in the top row (a–c). Comparison of experimental (black) and theoretical (green) spectra for nucleosides can be seen in panels d–f. Finally, experimental (black) and theoretical (blue) spectra for nucleotides are shown (g–i). For theoretical data, singly charged nucleotides as well as $H_2PO_4^{1-}$ are displayed due to complications that arise in the PCM treatment of doubly charged species (see text).

DOI: 10.1021/ja508149e
J. Am. Chem. Soc. 2015, 137, 201–209

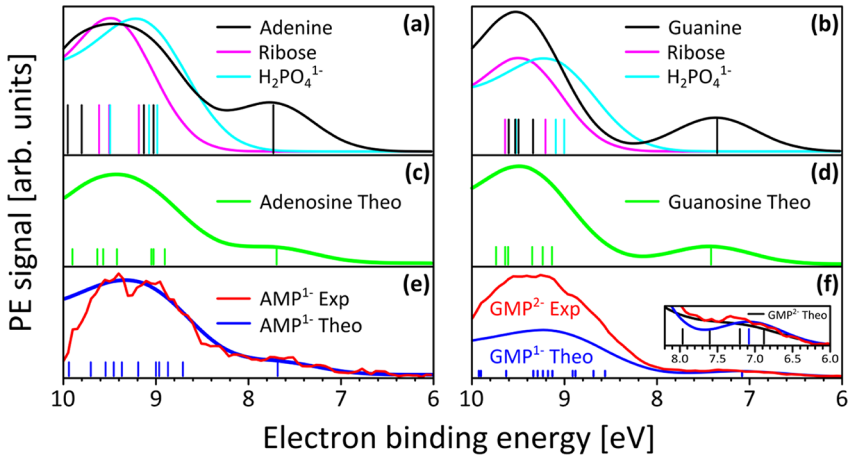

Figure 4. Decomposing the experimental and computed spectra for the purines. Computed spectra for nucleobases (black), pentose sugars (magenta), and singly charged phosphate (cyan) (a, b). $H_2PO_4^{1-}$ is shown instead of HPO_4^{2-} (see text). Panels c and d display computed (green) and stick spectra for purine nucleosides. No corresponding experimental data could be obtained due to solubility constraints. Experimental (red) and theoretical (blue) spectra of the purine nucleotide AMP^{1-} are seen in (e) and display very good agreement in the lowest energy peak position and overall shape. Panel f shows a comparison of the experimental spectrum for GMP^{2-} (red) to the theoretical spectrum for GMP^{1-} (blue). The inset panel provides a magnified view and includes the theoretical spectrum for GMP^{2-} (black). When black and blue curves are compared, it becomes apparent that there is an overestimation of the number of predicted ionization transitions for GMP^{2-} as compared to the number of predicted transitions for GMP^{1-}.

calculations for model compounds elsewhere.[39,46] Namely, we showed for ionization of neutral heteroaromatic species like imidazole that this approach gives accurate VIEs. The values, which are within a few tenths of an electronvolt below the experimental value, can be brought to even closer agreement with a hybrid approach combining microhydration by several explicit water molecules with NEPCM.[46] The microhydration approach is, however, impractical for the scope of the present calculations. As such, simulated spectra are generated by simply broadening the discrete lines from the calculated vertical ionization transitions by Gaussians with empirical fwhm = 1 eV, in agreement with the peak widths corresponding to single ionization transitions observed in several measured spectra.[32,37,46,47] Each transition is assumed to have an equal photoionization cross section as the energy of the ionizing photons is far above all ionization thresholds and the outgoing kinetic energy dependent cross sections are therefore assumed to be relatively slowly varying.

Computed spectra of the valence BE region of the pyrimidine nucleobases, pentose sugars, and phosphate ($H_2PO_4^{1-}$) can be seen in Figure 3a–c, along with sticks indicating the energies of individual ionization transitions. Each panel clearly illustrates that the lowest energy ionization transition originates from the nucleobase, is well-separated from other transitions, and occurs at BEs about 8 eV. All other transitions involving the sugar and phosphate, along with additional transitions from the nucleobase, occur at higher BEs of nearly 9 eV. There is one exception for cytosine, which has an additional ionizing transition at approximately 8.4 eV.

The theoretical results for the pyrimidine nucleosides strongly support what has already been deduced from the experimental data: the lowest BE spectral feature results from an ionization transition originating from an orbital located solely on the nucleobase. A direct comparison between the experimental and simulated spectra can be seen in Figure 3d–f. The lowest energy band is most clearly resolved in deoxythymidine, followed by uridine, and then cytidine. The calculations reveal that this is due to the larger energy gap between the first and second ionization transitions in deoxythymidine as compared to the energy gap in uridine (cytidine having the smallest energy gap). The second ionization transition of cytidine (at 8.4 eV) is a second low-lying ionization of the cytosine nucleobase (see the Supporting Information for the cytosine spectrum). In uridine and thymidine, a second transition originating from the nucleobase does not occur until 9.2 eV, as seen in Figure 3a–c. Although the simulations reproduce the band shapes and intensities well for the pyrimidine nucleosides, there is an offset in the calculations for the lowest VIE that is particularly noticeable in deoxythymidine (0.4 eV lower in the calculations). We argue that in this case the PCM probably does not describe the first solvation shell adequately.[32] In the Supporting Information we further discuss the role of microsolvation on the VIE.

For the nucleotides, both the calculated spectra (Figure 3g–i) and now also the lowest VIEs are in good agreement with experimental data. It is clear in all cases that the electron ejected from the HOMO originates from a base-centered orbital; however, molecular orbital assignments for more tightly bound electrons are less straightforward. For nucleosides, the higher BE band consists of transitions originating not only from orbitals located solely on the sugar and base but also from molecular orbitals that extend over both moieties. For nucleotides, the addition of the phosphate, whose spectral signature lies between that of the base and sugar, suggests that there are even more orbitals contributing to this higher BE spectral region. Representative examples of the molecular orbitals probed in the nucleotides are shown in the Supporting Information (Figure S9).

The simulated spectra for adenine and its nucleoside, as well as calculated and experimental AMP^{1-} results, are presented in Figure 4 together with the corresponding results from guanine and its derivatives. As for the pyrimidines, the purine nucleobases display a single ionization transition present at BEs < 9 eV. The lowest VIE for adenine is predicted to be 7.7 eV, only slightly less than those of the pyrimidine nucleobases. Guanine, however, has a calculated VIE value of 7.3 eV, well

DOI: 10.1021/ja508149e
J. Am. Chem. Soc. 2015, 137, 201–209

below that of all other nucleobases. The addition of a sugar results in no change in experimental VIE for the nucleoside adenosine compared to the VIE of its nucleobase, and only a minimal shift to 7.4 eV for guanosine. Figure 4e displays an excellent agreement between theory and experiment for the AMP^{1-} spectrum, as computations for monovalent nucleotides do not suffer from the same complications as those conducted for their divalent counterparts.[37] In Figure 4f, we therefore show the comparison of modeled spectra for monovalent GMP^{1-} with experimental results of GMP^{2-}. The agreement is very close at the onset of the spectrum but tends to be less satisfactory at higher energies where ionizations from the phosphate and sugar moieties appear. This latter issue as well as the limitations of the PCM model for divalent anions is discussed in greater detail in the Supporting Information, where experimental and calculated spectra for both the mono- and divalent forms of AMP are shown (Figure S5).

In an attempt to determine whether or not the identity of the counterion impacts the lowest VIE, we have further investigated computationally the effect of the association of Na^+ with the mono- and divalent forms of UMP and AMP. Calculations show that Na^+ in the vicinity of the phosphate group causes changes smaller than 0.1 eV, which is negligible given the width of the experimental peaks. This issue has been explored in detail in ref 37.

In all cases, nonequilibrium polarizable continuum calculations show there is a single ionization transition contributing to the lowest energy photoelectron band for all nucleobases, nucleosides, and nucleotides. Furthermore, this ionization originates solely from the nucleobase moiety. A summary of all theoretical and experimental results for the lowest band can be found in Table 3.

Reorganization Energies and Redox Potentials. So far our primary focus has been the analysis of VIEs obtained from the experimental PE peaks. As the lowest energy peak originates from a single ionizing transition, additional information can in principle be deduced from the peak width: the energy required for both the biomolecule and solvent to reorganize to relaxed geometries after the unit change in the nucleobase charge. The calculation of charge transport rates in oxidized DNA crucially depends on knowledge of this energetic parameter.[9,48] Direct knowledge of both the VIE and reorganization energy allows a determination of the one-electron standard reduction potential and represents an alternative to electrochemical experiments.

Photoionization of a neutral nucleoside results in the loss of an electron and the generation of an oxidized radical cation according to the half-reaction $N \rightarrow N^{\bullet+} + e^-$. The energy needed for the system to structurally relax from the original neutral position to that of the newly formed radical cation is the reorganization energy, λ.[10] This can be cast as the sum of two contributions, intramolecular (solute) λ_{in} and intermolecular (solvent) λ_{out}. In the limit of linear response, the PE peak width is related to the total λ through[49−51]

$$\sigma^2 = 2\lambda k_B T \quad (1)$$

where σ^2 corresponds to the variance of the Gaussian distributed spectral intensity, k_B is the Boltzmann constant, and T is the temperature. λ is readily accessible from computation as it corresponds to the free energy difference between the aqueous VIE and adiabatic ionization energy (AIE), with solute entropic contribution accounted for within the harmonic oscillator-free rotor approximation.

λ_{out} is estimated to be 1.1 eV for all four bases from the polarizable continuum model used here (Table 4). The fact that the λ_{out} values are the same within the error for all nucleosides may seem surprising at first sight. However, note that the solvent response is due to removal of a unit charge from the HOMO that is delocalized over the π system, the extent of which is roughly the same in all cases. A significantly higher value can be derived from previously simulated band profiles of thymine ionization.[52] These calculations used an effective fragment potential (EFP) and molecular dynamics for discrete solvent waters to capture the dynamical solvent structure at 300 K but kept the solute frozen ($\lambda_{in} = 0$).[52] Taking a Gaussian full width value of 0.75 eV from ref 52 allows an estimate via eq 1 of λ_{out} = 2.0 eV. As our calculations provide separately the internal reorganization energy of each solute, we can add this value to either of the theoretical estimates for the solvent relaxation. This now allows us to compare the overall reorganization energy thus computed with an experimental peak width.

Thymine in deoxythymidine is the system where the photoelectron spectra show the most clearly resolved lowest BE band, and therefore, it is the best current example to make this test. For this species, λ_{in} is 0.34 eV (Table 4) and yields, using the PCM solvent model, λ = 1.44 eV (from ref 32, Table 4) or, derived from the EFP solvent model,[52] λ = 2.3 eV. From these values, full peak widths predicted using eq 1 are 0.62 and 0.81 eV fwhm, respectively. The filled gray Gaussian in Figure 1a corresponds to fwhm = 0.62 eV. Gaussian fitting of the lowest binding energy experimental peak instead yields a fwhm of ∼0.9 eV. We note that widths in aqueous phase PE spectra broader than those expected from reorganizational grounds alone have been observed before.[28,49,53] We are therefore wary to discriminate between the quite different estimates for λ

Table 3. Summary of Lowest VIE Values (in eV) for Pentose Sugars, Phosphate, Nucleobases, Nucleosides, and Nucleotides

biomolecule	theory[a]	experiment[b]
ribose	9.2[c]	9.4
deoxyribose	9.1[c]	9.4
$H_2PO_4^{1-}$	9.0[c]	9.5[e]
HPO_4^{2-}	7.2[c]	8.9[e]
thymine	7.9[c]	
(d)thymidine	7.8[c]	8.1
$dTMP^{1-}$:$dTMP^{2-}$	7.7[c]:7.7[c]	
uracil	8.1	
uridine	8.0	8.1
UMP^{1-}:UMP^{2-}	8.0:7.9	−:8.0
cytosine	7.9[c]	
cytidine	7.8[c]	8.1
CMP^{1-}:CMP^{2-}	7.8[c]:7.7[c]	−:7.9
adenine	7.7[d]	
adenosine	7.7[d]	
AMP^{1-}:AMP^{2-}	7.7[d]:7.7	7.7:7.6
guanine	7.3[d]	
guanosine	7.4[d]	
GMP^{1-}:GMP^{2-}	7.1[d]:6.9	−:7.3

[a]PMP2/aug-cc-pVDZ with a NEPCM solvation model. [b]Experimental values for all nucleobase-containing molecules have an assigned error of ±0.1 eV. [c]In ref 32. [d]In ref 39. [e]In ref 37.

DOI: 10.1021/ja508149e
J. Am. Chem. Soc. 2015, 137, 201−209

Table 4. Comparing One-Electron Reduction Potentials (in eV) from Photoelectron Spectrum (PES) and Literature Electrochemical or Nanosecond Equilibrium Measurements[a]

nucleoside/ (nucleotide)	exptl VIE[b]	λ_{out}	λ_{in}	λ_{total}	$E^0(N^{\bullet+}/N)$ from PES vs SHE	$E^0(N^{\bullet+}/N)$ literature vs SHE[c,d]	E_7 vs SHE
deoxythymidine (dTMP)	8.1 (7.7*)	1.1 (1.0)	0.34 (0.53)	1.4 (1.6)	2.4 (1.9*)	2.11,[e] 1.90[h] (1.65[h])	~1.7[f] (1.45,[g] 1.63[l])
uridine (UMP)	8.1 (8.0)	1.1 (1.1)	0.21 (0.22)	1.3 (1.3)	2.5 (2.4)	≥2.39[e] (−)	
cytidine (CMP)	8.1 (7.9)	1.1 (1.1)	0.32 (0.6)	1.5 (1.7)	2.4 (1.9)	2.14,[e] 1.78[h] (1.68[h])	~1.6[f] (1.5,[g] 1.68[l])
adenosine (AMP)	7.7* (7.6)	1.1 (1.1)	0.27 (0.25)	1.4 (1.4)	2.1* (2.0)	1.96,[e] 1.61[h] (1.59[h])	1.44[i] (1.42,[g] 1.41[l])
guanosine (GMP)	7.4* (7.3)	1.1 (1.1)	0.44 (0.45)	1.5 (1.5)	1.6* (1.5)	1.49,[e] 1.47[j] (1.49[h])	1.29[k] (1.31,[g] 1.11[l])

[a]Values in parentheses are for nucleotides throughout. Reorganization energy values, λ, are computed from NEPCM vertical and PCM adiabatic ionization energies. E^0 from PES are determined by subtracting the theoretical reorganization energy from the experimental vacuum VIE and converting to SHE scale. Literature electrochemical E^0 for $N^{\bullet+} + e^- \rightarrow N$ relevant to the photoemission situation are directly available for nucleoside radical cations in acetonitrile (underlined). For water, reduction potentials vary with pH. The reduction potentials at pH 7 (E_7) reported from nanosecond equilibria are corrected to give $E^0(N^{\bullet+}/N)$ values (see Supporting Information). [b]From Table 3: experimental VIEs except (asterisk) where theoretical VIEs are used. [c]Reported standard state reduction potentials in ref 23 refer to fully protonated species in the redox couple, that is, $N^{\bullet+} + H^+ + e^- \rightarrow NH^+$. [d]$E^0$ for $N^{\bullet+} + e^- \rightarrow N$ calculated from original E_7 (or E_5/E_3 data) using experimental pK_a values quoted in ref 24; see the Supporting Information for details. [e]In ref 16. [f]Value for E_7 quoted in ref 23 unclear from cited reference how numbers determined.[59] [g]In ref 57. [h]E^0 have been recorrected from E_7 given in ref 23 using experimental pK_a values quoted in ref 24. See Supporting Information. Original E^0 values reported in ref 23 are 2.03 eV for adenosine and 1.58 eV for guanosine. [i]E^0 corrected from E_7 in ref 57 using experimental pK_a values quoted in ref 24. [j]Values in ref 23 for E_5 and E_3; value for E_7 is based on corrected extrapolation including deprotonation reaction of $Ado^{\bullet+}$. Original extrapolation in ref 23 yielded 1.42 V for adenosine. [k]E^0 corrected from E_7 from ref 23. [l]In ref 23. [m] In ref 58.

computed by the two theoretical approaches based on comparison with experimental peak widths alone.

A second approach to establish the correct magnitude of the solvent reorganization energy is to compare the VIE with the appropriate standard state redox potential for G, the only base for which the thermodynamic value is well-agreed upon.[23,24] $E^0(G^{\bullet+}/G)$, the standard state reduction potential for $G^{\bullet+}$, namely the negative of the free energy change for the reaction relevant to photoemission $G^{\bullet+}_{(aq)} + e^- \rightarrow G_{(aq)}$ at standard state, is simply the AIE referenced to the standard hydrogen electrode (SHE) rather than vacuum. If we compare our measured VIE for GMP (7.3 eV) with the literature $E^0(G^{\bullet+}/G)$, we can use λ = VIE − AIE to work backward to get a best estimate for λ_{out}. Furthermore, it is then reasonable to assume λ_{out} to be roughly the same for all systems. The most commonly cited[23] standard reduction potential for $G^{\bullet+}$, suitably converted here to $E^0(G^{\bullet+}/G)$ by carefully reconsidering protonation states (see Supporting Information), gives 1.5 V versus SHE. Taking into account the absolute half-cell potential for SHE relative to vacuum, 4.28 V,[24,54,55] the total reorganization energy, λ, for ionizing G is 7.3 − 1.5 − 4.3 = 1.5 eV.

This second line of evidence suggests that the PCM estimate for the solvent reorganization is quite accurate, with an error in λ (and, therefore, also in λ_{out}) of only ~0.2 eV. This is further supported by our test calculations on cytidine including 10 explicit water molecules within the PCM cavity (for more details see the Supporting Information), which yield λ larger by about 0.2 eV compared to the pure PCM value. We therefore choose to use the PCM model for the solvent response to ionization and leave rationalizing the observed experimental peak width for future work. We now have a route to derive the standard reduction potentials for the nucleobases other than G where it is much more poorly known. The best values found this way for the nucleoside and nucleotide radical cation standard reduction potentials $E^0(N^{\bullet+}/N)$ are shown in Table 4 using PE VIEs (where measured) and PCM values of the reorganization energies. The spread in VIEs (Tables 1 and 2) is essentially mapped onto the derived E^0 with U in uridine being the hardest to oxidize, $E^0(U^{\bullet+}/U)$ = 2.4 V, 1.0 V higher than G in GMP. For comparison, the most heavily cited $E^0(N^{\bullet+}/N)$ values in the literature are included in Table 4. These are Seidel et al.'s cyclic voltammetry results in aprotic acetonitrile[16] and Steenken and Jovanovic's redox parameters[23] obtained from measuring nanosecond equilibria in water. Note that the latter data for aqueous purines needed to be recalculated here. This is because for adenosine the equilibrium between its different protonation forms has not been properly taken into account in the original paper by Steenken and Jovanovic. For guanosine, a confused notation for E^0 in the same paper[23] has unfortunately propagated into a later study by Schlegel et al., which otherwise provides a very thorough analysis of issues connected with establishing redox potentials of DNA bases.[24] In particular, Schlegel and co-workers' research is important in that these authors carefully analyze the various equilibria for the radical cations, including the effect of specific[56] and long-range continuum solvation.[24] For direct comparison between original and recalculated data and discussion of corrections made here, see the Supporting Information and Table S2 therein. Another problem is that the experimental literature values are for nucleosides,[16,23] for which we have only data sets for pyrimidines. Due to purine nucleoside solubility constraints, the values shown for guanosine and adenosine in Table 4 use theoretically determined VIEs. But Fukuzumi et al., using a fast kinetics based approach similar to that of Steenken,[23] have more recently reported half-potentials at pH = 7 (E_7) for all the nucleotides.[57] These show that E_7 values are in fact very similar for the purine bases in nucleosides and nucleotides (see Table 4). Likewise, pulsed voltammetry shows oxidation at the same potential for nucleosides and nucleotides in the case of both pyrimidines and purines.[58]

In general, we find that it is possible to independently determine the standard reduction potentials by PE spectroscopy in water with assistance from ab initio calculations. The relative uncertainty in the redox potentials derived from photoelectron spectroscopy is sufficiently small to demonstrate that our E^0 values are in much better agreement with those values determined electrochemically in acetonitrile,[16] than with those from ref 23 that were obtained in water. On the basis of ~0.1 eV uncertainty in the determination of VIE, and

DOI: 10.1021/ja508149e
J. Am. Chem. Soc. 2015, 137, 201−209

experience with solvation of neutral and singly charged species employing the polarizable continuum model, the cumulative error may amount to as much as 0.2−0.3 eV in the *absolute* $E^0(N^{\bullet+}/N)$ values given in Table 4. However, we argue in the Supporting Information that the error in the computed reorganization energy is systematic; benchmarking with QM/MM calculations suggests that the reorganization energy is repeatedly underestimated by 0.2−0.25 eV. As such, the relative uncertainty in comparing one base to another is closer to 0.15 eV. Although this error exceeds that typical in electrochemical measurements, it allows us to independently establish a scale for the $E^0(N^{\bullet+}/N)$ in water in the absence of follow-up reactions (i.e., the direct oxidation reaction). Moreover, we show that the derived E^0 values align quantitatively with the nucleoside redox couples in acetonitrile. This conclusion is consistent with the findings of Schlegel and co-workers[24] who find small differences in values of $E^0(N^{\bullet+}/N)$ computed from first-principles in acetonitrile and water. We note that the spectroscopic scale of $E^0(N^{\bullet+}/N)$ that we propose here has even more positive values for deoxythymidine and cytidine than those measured by voltammetry in acetonitrile. This discrepancy could be attributable to a greater underestimation of the reorganization energy for a hole localized on single-ring aromatic compared to the more delocalized hole on an ionized purine.

CONCLUSIONS

We have measured the aqueous phase photoelectron spectra and have obtained the vertical ionization energies of the individual components of DNA, which include the pentose sugars, pyrimidine nucleosides and nucleotides, and purine nucleotides. The first vertical ionization energies for the aqueous pyrimidine nucleosides are essentially identical within experimental error. In nucleotides, the spectral contribution of the phosphate moiety can be seen at about 9 eV electron binding energy, consistent with previous photoelectron studies on aqueous divalent phosphate.[37] There is also little shift in the lowest VIE of the neutral pyrimidine nucleosides compared to the shift in doubly charged nucleotides. As expected, the VIEs for ionizing the purine group in their respective nucleotides are lower than in the corresponding pyrimidines. This lowering is particularly pronounced for GMP which is 0.7 V easier to vertically ionize than UMP.

Putting these results together, the photoelectron spectra of nucleic acid constituents can be viewed essentially as the sum over the component chemical groups. This is in strong contrast to the gas phase photoelectron spectra of nucleotides[31,33] and indicates that the solvent and the counterions effectively screen the charged phosphate moiety, thus preventing electrostatic interaction with the remainder of the molecule. The lack of spectral contributions at BEs less than 8 eV in the sugar and phosphate spectra[37] implies that the lowest BE peaks present in the nucleosides and nucleotides are due to the nucleobase. Although certainly an approximation, the nonequilibrium PCM model is shown to be effective in the treatment of solvent effects, and the resulting computed photoelectron spectra are in excellent agreement with experimental data. The electronic structure calculations confirm that the lowest energy feature is indeed due to a transition originating on the nucleobase in all cases.

Combining the experimental VIE measurements with the reorganization free energy λ values derived from the PCM model has allowed an independent spectroscopic determination of the one-electron E^0 values for these *aqueous* nucleic acid components, which does not suffer from follow-up reactions such as deprotonation that render electrochemical measurements irreversible. As a result, not only is the ordering of ease of oxidation among all the nucleobases confirmed but also the standard reduction potentials for the pyrimidine radical cations relative to the purine species are more firmly established. These standard reduction potentials should find use in more accurately parametrizing the kinetics of charge transfer in DNA, particularly as very recent PE spectra have shown rather negligible shifts in vertical ionization energies when the nucleobases are incorporated into the double helix.[28]

ASSOCIATED CONTENT

Supporting Information

Detailed information about the experimental methods, including sample preparation, sample structures (Figure S1), subtraction, normalization, and calibration (Figure S2) of the photoelectron spectra; differential photoelectron spectrum of cytosine for representative low-solubility nucleobase (Figure S3); protonation and phosphorylation of the adenine nucleotide (Figures S4 and S5); GMP concentration dependence on the PE spectrum, G-tetrad formation (Figure S6); theoretical description and calculations of the microsolvation within the NEPCM approach (Figure S7, S8, and S9); an exploration of the effect of microsolvation on the computed reorganization energy (Table S1); depiction of the four highest occupied molecular orbitals of all monovalent nucleotides in PCM water (Figure S10); description of the pH dependence of redox potentials (Figure S11); derivation of the prototropic equilibria and the reduction potential; extraction of the standard redox potentials from electrochemical literature for the nucleobases; correction of standard redox potential data for aqueous purines (Table S2). This material is available free of charge via the Internet at http://pubs.acs.org.

AUTHOR INFORMATION

Corresponding Authors

petr.slavicek@vscht.cz
bernd.winter@helmholtz-berlin.de
pavel.jungwirth@uochb.cas.cz
stephen.bradforth@usc.edu

Author Contributions

#C.A.S. and E.P. contributed equally to this work.

Notes

The authors declare no competing financial interest.

ACKNOWLEDGMENTS

We thank Professors Rich Roberts and Peter Qin for advice in biochemical preparation. The USC group is supported by the National Science Foundation under CHE-0957869 and CHE-1301465 and acknowledges the Helmholtz Zentrum Berlin for beam time. We also acknowledge Dr. Bernd Löchel and the Microtechnology group at BESSY for assistance with the HF preparations used in the course of the experimental work. P.J. thanks the Czech Science Foundation (grant P208/12/G016) and the Academy of Sciences (Praemium Academie Award). P.S. thanks the Czech Science Foundation (grant 13-34168S). E.P. thanks the International Max-Planck Research School for support and B.W. and R.S. acknowledge support from the Deutsche Forschungsgemeinschaft (projects WI 1327/3-1 and SE 2253/1-1).

DOI: 10.1021/ja508149e
J. Am. Chem. Soc. 2015, 137, 201−209

REFERENCES

(1) Lehnert, S. *Biomolecular Action of Ionizing Radiation (Series in Medical Physics and Biomedical Engineering)*, 1st ed.; Taylor & Francis: Boca Raton, FL, 2007.
(2) Morgan, W. F. *Radiat. Res.* **2003**, *159*, 581.
(3) Sutherland, B. M.; Bennett, P. V.; Sidorkina, O.; Laval, J. *Biochemistry* **2000**, *39*, 8026.
(4) Lomax, M. E.; Gulston, M. K.; O'Neill, P. *Radiat. Prot. Dosim.* **2002**, *99*, 63.
(5) O'Neill, M. A.; Barton, J. K. *Top. Curr. Chem.* **2004**, *236*, 67.
(6) Kawai, K.; Majima, T. *Acc. Chem. Res.* **2013**, *46*, 2616.
(7) Thazhathveetil, A. K.; Trifonov, A.; Wasielewski, M. R.; Lewis, F. D. *J. Am. Chem. Soc.* **2011**, *133*, 11485.
(8) Grozema, F. C.; Tonzani, S.; Berlin, Y. A.; Schatz, G. C.; Siebbeles, L. D. A.; Ratner, M. A. *J. Am. Chem. Soc.* **2009**, *131*, 14204.
(9) Marcus, R. A.; Sutin, N. *Biochim. Biophys. Acta* **1985**, *811*, 265.
(10) Wang, X.-B.; Wang, L.-S. *J. Chem. Phys.* **2000**, *112*, 6959.
(11) Bucher, D. B.; Pilles, B. M.; Carell, T.; Zinth, W. *Proc. Natl. Acad. Sci. U. S. A.* **2014**, *111*, 4369.
(12) Takaya, T.; Su, C.; de La Harpe, K.; Crespo-Hernandez, C. E.; Kohler, B. *Proc. Natl. Acad. Sci.* **2008**, *105*, 10285.
(13) Zhang, Y.; Dood, J.; Beckstead, A. A.; Li, X.-B.; Nguyen, K. V.; Burrows, C. J.; Improta, R.; Kohler, B. *Proc. Natl. Acad. Sci.* **2014**, *111*, 11612.
(14) Shapir, E.; Sagiv, L.; Molotsky, T.; Kotlyar, A. B.; Felice, R. D.; Porath, D. *J. Phys. Chem. C* **2010**, *114*, 22079.
(15) Porath, D.; Bezryadin, A.; de Vries, S.; Dekker, C. *Nature* **2000**, *403*, 635.
(16) Seidel, C. A.; Schulz, A.; Sauer, M. H. *J. Phys. Chem.* **1996**, *100*, 5541.
(17) Crespo-Hernández, C. E.; Close, D. M.; Gorb, L.; Leszczynski, J. *J. Phys. Chem. B* **2007**, *111*, 5386.
(18) Steenken, S. *Chem. Rev.* **1989**, *89*, 503.
(19) Yao, T.; Wasa, T.; Musha, S. *Bull. Chem. Soc. Jpn.* **1977**, *50*, 2917.
(20) Fiebig, T.; Wan, C.; Zewail, A. H. *ChemPhysChem* **2002**, *3*, 781.
(21) Heinze, J. *Angew. Chem., Int. Ed.* **1984**, *23*, 831.
(22) Guirado, G.; Fleming, C. N.; Lingenfelter, T. G.; Williams, M. L.; Zuilhof, H.; Dinnocenzo, J. P. *J. Am. Chem. Soc.* **2004**, *126*, 14086.
(23) Steenken, S.; Jovanovic, S. V. *J. Am. Chem. Soc.* **1997**, *119*, 617.
(24) Psciuk, B. T.; Lord, R. L.; Munk, B. H.; Schlegel, H. B. *J. Chem. Theory Comput.* **2012**, *8*, 5107.
(25) Sugiyama, H.; Saito, I. *J. Am. Chem. Soc.* **1996**, *118*, 7063.
(26) Bravaya, K. B.; Kostko, O.; Ahmed, M.; Krylov, A. I. *Phys. Chem. Chem. Phys.* **2010**, *12*, 2292.
(27) Cauët, E.; Valiev, M.; Weare, J. H. *J. Phys. Chem. B* **2010**, *114*, 5886.
(28) Pluhařová, E.; Schroeder, C.; Seidel, R.; Bradforth, S. E.; Winter, B.; Faubel, M.; Slavíček, P.; Jungwirth, P. *J. Phys. Chem. Lett.* **2013**, *4*, 3766.
(29) Trofimov, A. B.; Schirmer, J.; Kobychev, V. B.; Potts, A. W.; Holland, D.; Karlsson, L. *J. Phys. B: At. Mol. Phys.* **2005**, *39*, 305.
(30) Kim, N. S.; LeBreton, P. R. *J. Am. Chem. Soc.* **1996**, *118*, 3694.
(31) Yang, X.; Wang, X.-B.; Vorpagel, E. R.; Wang, L.-S. *Proc. Natl. Acad. Sci. U. S. A.* **2004**, *101*, 17588.
(32) Slavíček, P.; Winter, B.; Faubel, M.; Bradforth, S. E.; Jungwirth, P. *J. Am. Chem. Soc.* **2009**, *131*, 6460.
(33) Chatterley, A. S.; Johns, A. S.; Stavros, V. G.; Verlet, J. R. R. *J. Phys. Chem. A* **2013**, *117*, 5299.
(34) Faubel, M.; Schlemmer, S.; Toennies, J. P. *Z. Phys. D: At., Mol. Clusters* **1988**, *10*, 269.
(35) Wilson, K. R.; Rude, B. S.; Smith, J.; Cappa, C.; Co, D. T.; Schaller, R. D.; Larsson, M.; Catalano, T.; Saykally, R. J. *Rev. Sci. Instrum.* **2004**, *75*, 725.
(36) Winter, B.; Faubel, M. *Chem. Rev.* **2006**, *106*, 1176.
(37) Pluhařová, E.; Ončák, M.; Seidel, R.; Schroeder, C.; Schroeder, W.; Winter, B.; Bradforth, S. E.; Jungwirth, P.; Slavíček, P. *J. Phys. Chem. B* **2012**, *116*, 13254.
(38) Winter, B.; Weber, R.; Hertel, I. V.; Faubel, M.; Jungwirth, P.; Brown, E. C.; Bradforth, S. E. *J. Am. Chem. Soc.* **2005**, *127*, 7203.
(39) Pluhařová, E.; Jungwirth, P.; Bradforth, S. E.; Slavíček, P. *J. Phys. Chem. B* **2011**, *115*, 1294.
(40) Frisch, M. J.; Trucks, G. W.; Schlegel, H. B.; Scuseria, G. E.; Robb, M. A.; Cheeseman, J. R.; Montgomery, J. A., Jr.; Vreven, T.; Kudin, K. N.; Burant, J. C.; Millam, J. M.; Iyengar, S. S.; Tomasi, J.; Barone, V.; Mennucci, B.; Cossi, M.; Scalmani, G.; Rega, N.; Petersson, G. A.; Nakatsuji, H.; Hada, M.; Ehara, M.; Toyota, K.; Fukuda, R.; Hasegawa, J.; Ishida, M.; Nakajima, T.; Honda, Y.; Kitao, O.; Nakai, H.; Klene, M.; Li, X.; Knox, J. E.; Hratchian, H. P.; Cross, J. B.; Bakken, V.; Adamo, C.; Jaramillo, J.; Gomperts, R.; Stratmann, R. E.; Yazyev, O.; Austin, A. J.; Cammi, R.; Pomelli, C.; Ochterski, J. W.; Ayala, P. Y.; Morokuma, K.; Voth, G. A.; Salvador, P.; Dannenberg, J. J.; Zakrzewski, V. G.; Dapprich, S.; Daniels, A. D.; Strain, M. C.; Farkas, O.; Malick, D. K.; Rabuck, A. D.; Raghavachari, K.; Foresman, J. B.; Ortiz, J. V.; Cui, Q.; Baboul, A. G.; Clifford, S.; Cioslowski, J.; Stefanov, B. B.; Liu, G.; Liashenko, A.; Piskorz, P.; Komaromi, I.; Martin, R. L.; Fox, D. J.; Keith, T.; Al-Laham, M. A.; Peng, C. Y.; Nanayakkara, A.; Challacombe, M.; Gill, P. M. W.; Johnson, B.; Chen, W.; Wong, M. W.; Gonzalez, C.; Pople, J. A. *Gaussian 03*, Revision E.01; Gaussian, Inc.: Wallingford, CT, 2004.
(41) *Thermodynamics Data for Biochemistry and Biotechnology*, 1st ed.; Hinz, H.-J., Ed.; Springer-Verlag: Berlin, Germany, 1986.
(42) Buchner, F.; Ritze, H.-H.; Lahl, J.; Lübcke, A. *Phys. Chem. Chem. Phys.* **2013**, *15*, 11402.
(43) Yalkowsky, S. H. *Handbook of Aqueous Solubility Data*, 1st ed.; CRC Press: Boca Raton, FL, 2003.
(44) Lide, D. R. *CRC Handbook of Chemistry and Physics*, 81st ed.; CRC Press: Boca Raton, FL, 2000.
(45) Neurohr, K. J.; Mantsch, H. H. *Can. J. Chem.* **1979**, *57*, 1986.
(46) Jagoda-Cwiklik, B.; Slavíček, P.; Cwiklik, L.; Nolting, D.; Winter, B.; Jungwirth, P. *J. Phys. Chem. A* **2008**, *112*, 3499.
(47) Ghosh, D.; Roy, A.; Seidel, R.; Winter, B.; Bradforth, S. E.; Krylov, A. I. *J. Phys. Chem. B* **2012**, *116*, 7269.
(48) Marcus, R. A. *J. Chem. Phys.* **1965**, *43*, 679.
(49) Seidel, R.; Faubel, M.; Winter, B.; Blumberger, J. *J. Am. Chem. Soc.* **2009**, *131*, 16127.
(50) Blumberger, J. *Phys. Chem. Chem. Phys.* **2008**, *10*, 5651.
(51) Tateyama, Y.; Blumberger, J.; Sprik, M.; Tavernelli, I. *J. Chem. Phys.* **2005**, *122*, 234505.
(52) Ghosh, D.; Isayev, O.; Slipchenko, L. V.; Krylov, A. I. *J. Phys. Chem. A* **2011**, *115*, 6028.
(53) Seidel, R.; Thürmer, S.; Moens, J.; Geerlings, P.; Blumberger, J.; Winter, B. *J. Phys. Chem. B* **2011**, *115*, 11671.
(54) Truhlar, D. G.; Cramer, C. J.; Lewis, A.; Bumpus, J. A. *J. Chem. Educ.* **2007**, *84*, 934.
(55) Donald, W. A.; Williams, E. R. *Pure Appl. Chem.* **2011**, *83*, 2129.
(56) Thapa, B.; Schlegel, H. B. *J. Phys. Chem. A* **2014**, DOI: 10.1021/jp5088866.
(57) Fukuzumi, S.; Miyao, H.; Ohkubo, K.; Suenobu, T. *J. Phys. Chem. A* **2005**, *109*, 3285.
(58) Oliveira-Brett, A. M.; Piedade, J. A. P.; Silva, L. A.; Diculescu, V. C. *Anal. Biochem.* **2004**, *332*, 321.
(59) Jovanovic, S. V.; Simic, M. G. *J. Phys. Chem.* **1986**, *90*, 974.

DOI: 10.1021/ja508149e
J. Am. Chem. Soc. 2015, 137, 201−209